[CANCER RESEARCH 62, 5603–5610, October 1, 2002]

Mice Lacking the EDB Segment of Fibronectin Develop Normally but Exhibit Reduced Cell Growth and Fibronectin Matrix Assembly *in Vitro*[1]

Tomohiko Fukuda,[2] Nobuaki Yoshida,[3] Yuki Kataoka,[3] Ri-ichiroh Manabe, Yoko Mizuno-Horikawa, Motohiko Sato, Kohji Kuriyama, Natsuo Yasui,[4] and Kiyotoshi Sekiguchi[5]

Institute for Protein Research [T. F., Y. M-H., K. S.] and Department of Orthopedic Surgery, Faculty of Medicine [M. S., K. K., N. Ya.], Osaka University, Suita, Osaka 565-0871; Research Institute, Osaka Medical Center for Maternal and Child Health, Izumi, Osaka 594-1011 [T. F., N. Yo., Y. K., R. M., K. S.]; and Sekiguchi Biomatrix Signaling Project, Japan Science and Technology Corporation, Nagakute, Aichi 480-1195 [R. M., K. S.], Japan

ABSTRACT

Fibronectins (FNs) are major cell-adhesive proteins in the extracellular matrix and are essential for embryonic development. FNs are encoded by a single gene, but heterogeneity is introduced by alternative pre-mRNA splicing. One of the alternatively spliced segments, extra domain B (EDB), is prominently expressed during embryonic development and in tumor tissues, although it is mostly eliminated from FN in normal adult tissues. To examine the function of the EDB segment *in vivo*, we generated mice lacking the EDB exon using the Cre-loxP system. Although EDB-containing FNs are highly expressed throughout early embryogenesis, EDB-deficient mice developed normally and were fertile. Despite the absence of any significant phenotypes observed *in vivo*, however, fibroblasts obtained from EDB-deficient mice grew slowly *in vitro* and deposited less FN in the pericellular matrix than fibroblasts from wild-type mice. These results indicate that expression of EDB-containing isoforms is dispensable during embryonic development, yet may play a modulating role in the growth of connective tissue cells via the FN matrix.

INTRODUCTION

FNs[6] are multifunctional glycoproteins present in the extracellular matrix as insoluble components or in circulating plasma as soluble proteins. FNs are adhesive proteins playing major roles in the adhesion, migration, differentiation, and proliferation of cells and have been implicated in wound healing and embryonic development (1). Disruption of the FN gene in mice results in an embryonic lethality, confirming the importance of FN in embryonic development (2, 3). FNs consist of three types of homologous repeating units, types I, II, and III (4). Type I and type II repeats are clustered in the NH_2-terminal and COOH-terminal parts of the molecule, whereas type III repeats are clustered in the central part. These repeats are organized into a series of functional domains that bind to collagens, heparin and heparan sulfate, fibrin, the integrin family of cell adhesion receptors, and FNs themselves.

FNs exhibit molecular heterogeneity arising from alternative splicing of a primary transcript at three distinct regions termed EDA, EDB, and IIICS (5–8). Two type III repeats, EDA and EDB, are either included or excluded from FN mRNA by exon skipping (8). Alternative splicing at the EDA and EDB regions is regulated in a tissue-specific and developmental stage-dependent manner. FNs expressed in fetal tissues contain a greater percentage of the EDA and EDB segments than those expressed in adult tissues (9–13). In mice, FNs lacking the EDA and EDB segments are expressed in many adult tissues, although FNs containing either EDA or EDB segments are expressed in restricted tissues such as blood vessels and lung interstitium (EDA-containing FNs) and cartilage and cornea (EDB-containing FNs; Ref. 14).

Despite accumulating evidence for the regulated expression of EDA- and/or EDB-containing FNs *in vivo*, the biological functions of these isoforms are poorly understood. Recently, we showed that the EDA segment regulates the binding affinity of FNs for integrin $\alpha5\beta1$ and thereby stimulates integrin-mediated signal transduction and subsequent cell cycle progression (15, 16). The EDA segment was also shown to stimulate the conversion of hepatic lipocytes to myofibroblast-like cells (17) and cytokine-dependent matrix metalloproteinase expression (18), although the molecular basis of these phenomena remain to be elucidated. Unlike the EDA segment, the EDB segment did not enhance FN binding to integrin $\alpha5\beta1$ (15, 16) or stimulate myofibroblast conversion of lipocytes (17), but it was more readily incorporated into the extracellular matrix (19). The amino acid sequence of the EDB segment is 100% identical for human, rat, and mouse. Even between human and chicken, the identity of this amino acid sequence is as high as 97%. Given that EDB is selectively expressed during embryonic development, wound healing, and malignant transformation, the exceptionally high sequence homology of EDB may imply that it has an important function in these biological processes.

One approach to elucidate the hitherto unknown functions of EDB, particularly those *in vivo*, is to generate mice in which the EDB exon has been deleted from the FN gene. To generate such mice, we used the Cre-loxP system of the bacteriophage P1 (20) to excise the EDB exon from the FN gene together with the selection marker cassette which had been introduced to isolate the homologously recombined ES cells. Surprisingly, the homozygous EDB-deficient mice were apparently normal and fertile, although the fibroblasts obtained from the homozygous mice exhibited reduced potential for cell growth and FN matrix assembly *in vitro*.

MATERIALS AND METHODS

Construction of the Targeting Vector. A 14 kb genomic clone containing the exon EDB was isolated from a FIX-II 129/Sv mouse genomic DNA library (Stratagene, La Jolla, CA), using the mouse FN cDNA encoding the EDB segment as a probe. The genomic clone was mapped for the major restriction enzyme sites and used to construct the targeting vector. A gene cassette containing the neomycin-resistance (*neo*) gene flanked by two loxP sites (a generous gift of Dr. Klaus Rajewsky, University of Cologne, Cologne, Germany) was inserted into the intron between the exons III7b and EDB at *Nde*I sites, and a third loxP site was also inserted into the intron between the exons EDB and III8a at an *Apa*I site using PCR (Fig. 1). A gene cassette containing the herpes simplex virus thymidine kinase gene, which was also kindly

Received 4/25/02; accepted 7/30/02.

The costs of publication of this article were defrayed in part by the payment of page charges. This article must therefore be hereby marked *advertisement* in accordance with 18 U.S.C. Section 1734 solely to indicate this fact.

[1] Supported by Special Coordination Funds from Science and Technology Agencies of Japan (to K. S.) and Grants-in-Aid from Ministry of Education, Culture, Sports, Science, and Technology of Japan (to K. S., T. F.).

[2] Present address: Department of Pathology, University of Pittsburgh, 715 Scaife Hall, Pittsburgh, PA 15213.

[3] Present address: The Institute of Medical Science, The University of Tokyo, 4-6-1 Shirokanedai, Minato-ku, Tokyo 108-8639, Japan.

[4] Present address: Department of Orthopedic Surgery, The University of Tokushima, Tokushima 770-8503, Japan.

[5] To whom requests for reprints should be addressed, at Institute for Protein Research, Osaka University, 3-2 Yamadaoka, Suita, Osaka 565-0871, Japan. Phone: 81-6-6879-8617; Fax: 81-6-6879-8619; E-mail: sekiguch@protein.osaka-u.ac.jp.

[6] The abbreviations used are: FN, fibronectin; FBS, fetal bovine serum; PMSF, phenylmethylsulfonyl fluoride; EDA, extra domain A; EDB, extra domain B; IIICS, type III-connecting segment.

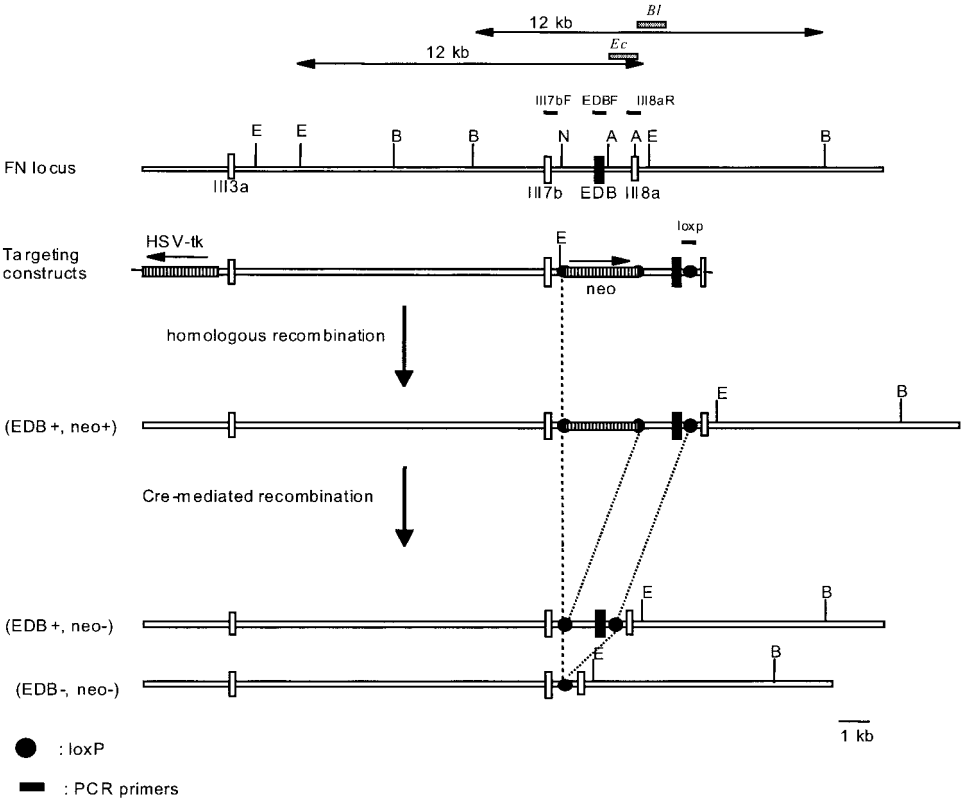

Fig. 1. Strategy for targeting of the EDB exon. Restriction maps of the mouse FN gene encompassing exons III3a through III8a, the targeting vector, the targeted allele after homologous recombination, and the targeted alleles with or without the EDB exon after Cre-mediated excision are shown. The targeting vector was designed to insert a floxed *neo* gene into the intron between the III7b and EDB exons, and a third loxP site into the intron between the EDB and III8a exons. After homologous recombination, ES cells were transiently transfected with a plasmid encoding the Cre enzyme, which resulted in the removal of the exon EDB and/or *neo* gene, leaving a single loxP site behind. Homologously recombined ES clones and those after Cre-mediated recombination were identified by Southern blot analysis as detailed in Fig. 2. Briefly, homologously recombined clones gave rise to a 4.5-kb fragment upon *Eco*RI digestion of genomic DNA and a 14.5-kb fragment upon *Bln*I digestion, whereas Cre-mediated recombinant clones with or without the EDB exon gave rise to 2.3-kb and 1.2-kb fragments upon *Eco*RI digestion, respectively, and 12.0-kb and 10.5-kb fragments upon *Bln*I digestion. HSV-tk, herpes simplex virus thymidine kinase.

provided by Dr. K. Rajewsky, was then introduced 5′ to the mouse FN genomic DNA for negative selection.

Generation of EDB-deficient Mice. E14.1 ES cells (5×10^6) were transfected with 30 μg of the targeting construct by electroporation. The transfected cells were grown on irradiated mouse embryonic fibroblasts and selected in the presence of G418 (400 μg/ml) and Gancyclovir (2 μM). Homologously recombined clones were identified by PCR using the following primers: 5′-AAGACGGGGATAACTTCGTATAATGTATGC-3′ (designated 'loxP') designed after the loxP sequence and its 3′ intronic sequence between the exons EDB and III8a; and 5′-GTCCTCTTCATTCTTCACGGGTGAGTAGCG-3′ (designated 'III8aR') taken from the intronic sequence 3′ to the exon III8a, which is absent from the targeting vector (Fig. 1). These primers generate a 1.2 kb fragment from successfully targeted cells. Targeted cells were verified by Southern blot analysis of the *Bln*I digest of genomic DNA using a probe covering the 3′ region of exon III8a and its 3′ intronic sequence (designated 'Bl'; Fig. 1). The homologously recombined clones were then transfected with pIC-Cre (a gift from Dr. K. Rajewsky; Gu *et al.,* Ref. 21) and grown on irradiated mouse embryonic fibroblasts at a low cell density (1×10^3 cells/10-cm dish) to allow transfected cells to form colonies. The colonies were individually picked up and expanded in duplicate 24-well plates, one of which was fed with medium containing G418 to select transfected cells from which the *neo* cassette had been deleted by Cre recombinase. G418-sensitive clones were screened for Cre-mediated deletion of the EDB exon by Southern blot analysis of the *Eco*RI digest of genomic DNA using a probe covering the intron between the EDB exon and exon III8a and 5′ region of exon III8a (designated 'Ec'). The clones, yielding a 1.2-kb band, were expanded and injected into C57BL/6 blastocysts. Male chimeric mice were mated with 129/Svter females to obtain heterozygous (*i.e.,* $EDB^{+/-}$) mice. Mice were genotyped by PCR using the following pairs of primers: (*a*) 5′-CCAGATATCACTGGCTACAGAATAACTACT-3′ (primer III7bF), which was positioned within exon III7b and the primer III8aR; and (*b*) 5′-GAGGTGCCCCAGCTCACTGACCTAAGC-3′ (primer EDBF), which was positioned within the EDB exon and the primer III8aR. DNA from tail biopsies was isolated by proteinase K digestion followed by isopropanol precipitation.

Isolation of Extracellular Matrix from Cultured Fibroblasts. Mouse embryonic fibroblasts were grown in DMEM supplemented with 10% FN-depleted FBS in 10-cm dishes. FN-depleted FBS was prepared by passing the FBS through a gelatin affinity column twice. The FN-containing extracellular matrix was prepared from cells that had been kept in culture for 3 days after they had reached confluency (22) with a slight modification. Briefly, the cell layers were rinsed three times with PBS at room temperature and lysed twice 10 min each in 50 mM Tris-HCl (pH 8.0) containing 0.5% sodium deoxycholate, 1 mM PMSF, 1 mM EDTA, and 145 mM NaCl at 4°C on a slowly moving four-way shaker. The resulting insoluble matrices were washed twice with low ionic strength buffer [2 mM Tris-HCl (pH 8.0), containing 1 mM PMSF, and 1 mM EDTA], twice with high ionic strength buffer [20 mM Tris-HCl (pH 8.0), containing 1 mM PMSF, 1 mM EDTA, 1 M NaCl], and finally twice with low ionic strength buffer again at 4°C. The remaining FN-containing matrices were recovered in 1 ml of 10 mM Tris-HCl (pH 6.8) containing 0.1% SDS, 50 mM NaCl, and 0.5 mM EDTA, lyophilized, and analyzed by immunoblotting as described below.

SDS-PAGE and Immunoblot Analysis. SDS-PAGE of purified FNs or isolated extracellular matrices were performed as described by Laemmli (23) using 6% polyacrylamide gels under reducing conditions. The separated proteins were transferred to nitrocellulose membranes and probed with polyclonal antibodies against human plasma FN (24) or against the EDB segment of mouse FN. The anti-EDB antibody was raised in rabbits by immunization with a mixture of two synthetic peptides, EGIIFEDFVDSSVGY and YTVTGLEPGIDYDIS, after conjugation to keyhole limpet hemocyanin by the glutaraldehyde method (25). The specificity of the anti-EDB antibody was verified by immunoblot analysis using recombinant human FN containing the EDB segment (15). The bound antibodies were visualized with peroxidase-linked goat antibodies against rabbit IgG using the enhanced chemiluminescence system (Amersham Corp., Arlington Heights, IL). Recombinant human FNs containing both EDA and EDB as well as plasma FN were purified as described previously (15).

Histological Examination. Knee joint tissues from newborn, 5-week- and 6-month-old mice were fixed in 4% paraformaldehyde, decalcified in EDTA, dehydrated with ethanol, and embedded in paraffin. Sections (4-μm thick) were stained with H&E. For the experimental model of fracture healing, the right eighth ribs of 5-week-old mice were fractured by surgery under anesthesia as described previously (26). The mice were sacrificed on the seventh day after fracture, and the process of fracture healing was examined histologically.

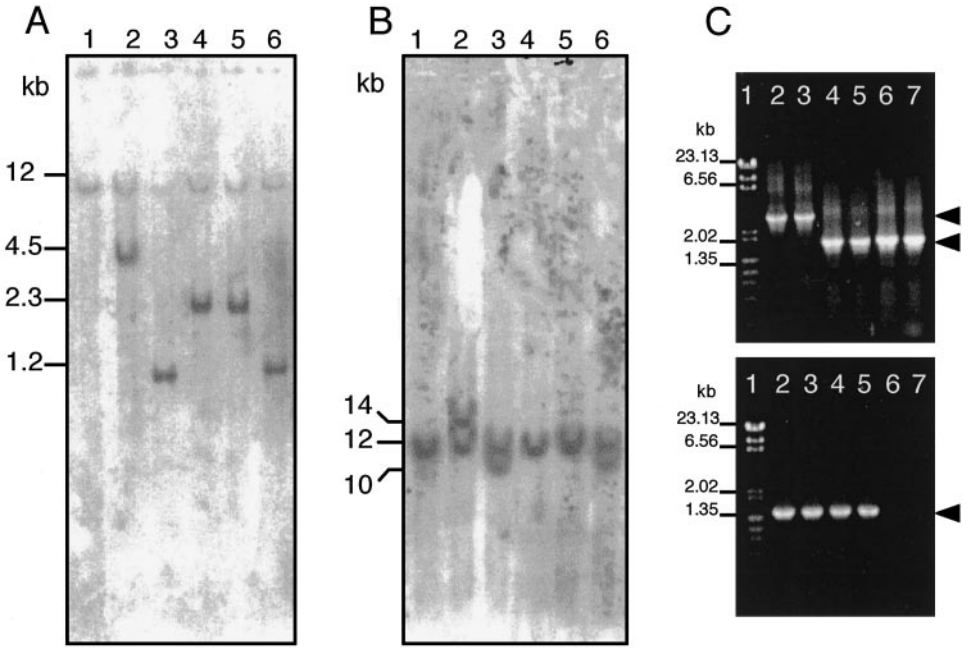

Fig. 2. Identification of targeted ES cells by Southern blot analysis. Southern blot analysis of genomic DNA from ES clones was performed after *Eco*RI (*A*) or *Bln*I (*B*) digestion. Positions of the probes used (*Ec* and *Bl*) are shown in Fig. 1. *Lane 1*, wild-type ES cells; *Lane 2*, ES clone no. 74 obtained after homologous recombination; *Lanes 3* and *6*, ES clones with the EDB exon deleted by Cre-mediated recombination; *Lanes 4* and *5*, ES clones with retained EDB exon after Cre-mediated recombination. Genotypes of offspring obtained by crossing of mice heterozygous for the EDB-deleted allele were determined by PCR using two different pairs of primers, *i.e.*, III7bF/III8aR (*top panel*; *C*) and EDBF/III8aR (*bottom panel*). *Lane 1*, DNA size markers; *Lanes 2* and *3*, wild-type mice; *Lanes 4* and *5*, heterozygous mice; and *Lanes 6* and *7*, homozygous mice. Note that no PCR fragment was amplified from homozygous mice with the EDBF/III8aR primers, confirming the absence of the EDB exon from both alleles encoding FN. It was also noted that the 3-kb fragment was not significantly amplified from the wild-type allele of heterozygous mice, possibly because PCR is biased in favor of amplification of shorter fragments.

Sections of other tissues were processed as described above, except that the decalcification step was omitted.

Quantitation of FNs in Plasma and Culture Medium. Blood (0.5 ml) was drawn from the mouse tail vein into a syringe containing a 25-μl aliquot of 0.2 M EDTA (pH 7.5). Plasma was separated from blood cells by centrifugation at 20,000 $\times$ *g* for 30 s and snap-frozen in small aliquots. All assays were performed on freshly thawed aliquots. The concentration of FNs in plasma was measured by ELISA, using collagen type I-coated 96-well polystyrene plates (Iwaki Glass, Tokyo, Japan) to capture the FNs, and a polyclonal antimouse FN antibody (Biogenesis, Poole, United Kingdom) to quantify captured FNs. The FN concentration in the conditioned medium of cultured fibroblasts was also measured by ELISA as described above.

Immunofluorescence Staining of FN Matrix. Mouse embryonic fibroblasts were cultured in DMEM containing 10% FBS and 2 mM glutamine and harvested with 0.025% trypsin/1 mM EDTA. Cells (2×10^5) were plated onto glass coverslips placed in 24-well culture plates and cultured for 24 h in DMEM containing 5% FN-depleted FBS and 2 mM glutamine. Cells were then fixed with 3.7% formaldehyde for 10 min at room temperature and stained with the polyclonal anti-mouse FN antibody for 1 h at room temperature, followed by incubation with a FITC-labeled secondary antibody for immunofluorescence detection. Stained cells were observed using a Zeiss Axioplan fluorescence microscope, and representative fields were photographed using Kodak Ektachrome 400$\times$ film. Densitometric quantitation of the fluorescence intensities of FN matrix was performed using the public domain NIH Image program developed at the United States National Institute of Health and available on-line.[7]

Cell Growth Assay. Mouse fibroblasts prepared from the embryos of knockout mice were cultured in DMEM containing 10% FBS and 2 mM glutamine and harvested with 0.025% trypsin/1 mM EDTA. Cells (1.5×10^4) were plated on 35-mm culture dishes and cultured in DMEM containing 5% FN-depleted FBS and 2 mM glutamine at 37°C under a 5% CO_2/95% air atmosphere. Cells were harvested with 0.025% trypsin/1 mM EDTA, and the cell number was determined using a Coulter counter model Z1.

RESULTS

Generation of EDB-deficient Mice. We deleted the EDB exon from the mouse FN gene using the Cre-loxP system of bacteriophage P1. A FIX-II 129/Sv mouse genomic library was screened with a cDNA probe encoding the EDB segment. One of the clones thus obtained, clone no. 122, was mapped for its restriction sites (Fig. 1) and used to construct the targeting vector as follows. A *neo* gene flanked by two loxP sites was inserted into the intron between exons III7b and EDB for positive selection, and a third loxP site was inserted into the intron between exons EDB and III8a. A herpes simplex virus-thymidine kinase gene was placed 5′ to exon III3a for negative selection (Fig. 1). The linearized targeting vector was transfected into E14.1 ES cells by electroporation, and the cells were subjected to positive selection with G418 and negative selection with Gancyclovir. Clones containing the homologously recombined allele were identified by PCR and Southern blot analysis. These clones produced 4.5-kb and 14.5-kb bands upon Southern blots of *Eco*RI and *Bln*I digests of genomic DNA (Fig. 2, *A* and *B*; *Lane 2*). Approximately 5% of the selected clones were positive for homologous recombination.

The ES cells containing the targeted allele were transfected with a Cre-encoding plasmid to excise the floxed EDB exon and *neo* cassette. Cre-mediated recombination was expected to yield three distinct types of deletion, *i.e.*, deletion of either exon EDB or the neo cassette alone or deletion of both. The deletion retaining the *neo* gene could be distinguished from the other types of deletion upon selection with G418 because ES cells lacking the *neo* gene cannot survive G418 treatment. Southern blot analysis of the G418-sensitive clones identified two groups of clones: those yielding a 2.3-kb band with *Eco*RI-digested DNA and a 12-kb band with *Bln*I-digested DNA (Fig. 2, *A* and *B*; *Lanes 4* and *5*), indicative of the presence of the EDB exon; and those yielding a 1.2-kb band with *Eco*RI digest and a 10-kb band with *Bln*I digest (Fig. 2, *A* and *B*; *Lanes 3* and *6*), indicative of the deletion of the EDB exon. Eighty-five percent of the G418-sensitive clones scored positive for Cre-mediated recombination. Two independent clones containing the EDB-deleted allele were injected to C57BL/6 blastocysts and used to generate chimeric males, of which four males were found to be capable of transmitting the targeted allele to their progeny. Mice heterozygous for the deleted EDB exon were identified by PCR using the primer pair III7bF/III8aR (Fig. 2*C*); wild-type mice gave rise to a 3 kb-fragment, whereas heterozygous mice produced only a 1.7-kb fragment. Failure to detect the 3-kb fragment in the PCR products of heterozygous mice could be because of a bias toward smaller fragments in PCR amplification of multiple-sized fragments with a single primer pair, thus resulting in a prefer-

[7] Internet address: rsb.info.nih.gov/nih-image/.

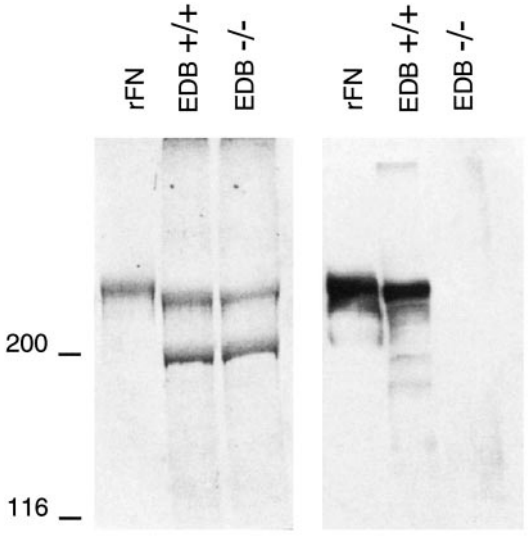

Fig. 3. SDS-PAGE and immunoblot analyses of FN-containing matrix. FN-containing extracellular matrix was prepared from wild-type ($EDB^{+/+}$) and $EDB^{-/-}$ embryonic fibroblasts that had been grown in culture medium supplemented with FN-deficient FBS (see "Materials and Methods") and subjected to SDS-PAGE under reducing conditions, followed by Coomassie Blue staining (*left*) or by immunoblotting with an anti-EDB antibody (*right*). Recombinant FN containing both EDA and EDB segment (*rFN*; *left lane* of each *panel*) was included as a positive control for EDB-containing FN. Shown in the margin are the positions of molecular weight markers.

ential amplification of the 1.7-kb fragment with respect to the 3-kb fragment. In support of this possibility, PCR using another pair of primers, *i.e.*, EDBF/III8aR, yielded a 1.5-kb fragment from both wild-type and heterozygous mice, demonstrating that the wild-type allele was present in heterozygous mice. Intercrossing of heterozygous mice produced offspring homozygous for the EDB-deleted allele, yielding a 1.7-kb fragment with the III7bF/III8aR primer pair but no 1.5-kb fragment with EDBF/III8aR (Fig. 2*C*; *Lanes 6* and *7*).

EDB-deficient Mice Are Apparently Normal. Mice heterozygous for the targeted FN allele appeared healthy and were approximately the same size as their wild-type littermates. Although the EDB-containing FNs are highly expressed throughout early embryonic development, intercrossing heterozygous mice produced homozygous $EDB^{-/-}$ offspring at an expected Mendelian frequency (*i.e.*, the numbers of wild-type, heterozygous, and homozygous mice were 84, 167, 77, respectively, indicating that lack of the EDB exon does not cause embryonic lethality). These mice developed apparently normally and were fertile. No apparent abnormalities were observed in homozygous mice upon anatomical inspection of major organs. Despite the proposed role of EDB-containing FN as an angiogenesis marker (27, 28), the lung and kidney, two major organs with extensive microvasculature, did not show any noticeable anatomical abnormality with respect to vasculogenesis (data not shown). The concentration of FN in blood plasma was 418 ± 92 μg/ml in wild-type mice, 441 ± 40 μg/ml in heterozygous mice and 472 ± 93 μg/ml in homozygous mice, demonstrating that the deletion of the EDB exon did not perturb the expression of the FN gene either at the transcription or translation level.

To confirm the absence of EDB-containing FNs in homozygous mice, fibroblasts were isolated from embryos of wild-type, heterozygous, and homozygous mice and examined for the expression of EDB-containing FNs. Confluent monolayers of these fibroblasts were extracted with 0.5% sodium deoxycholate, and the resulting insoluble matrices were analyzed by immunoblotting with an antibody specifically recognizing the EDB segment (Fig. 3). Although FNs were deposited in the matrices of both wild-type and $EDB^{-/-}$ fibroblasts, EDB-containing FNs were only detectable in the matrix of the wild-type fibroblasts, confirming the inability of the homozygous mice to produce EDB-containing FNs. It was also noted that the intensity of the FN band (Fig. 3, *left panel*) was less pronounced in the matrix from $EDB^{-/-}$ fibroblasts, suggesting that EDB-deficient FNs have reduced ability to assemble into the extracellular matrix.

Cartilage Development in EDB-deficient Mice. In normal adult mice, EDB-containing FNs are expressed only in restricted tissues such as hyaline cartilage and Descemet's membrane of cornea (14). EDB-containing FNs may thus have a role in the development and/or maintenance of these tissues. In search of any morphological aberration in EDB-deficient mice, we compared the histology of the hyaline cartilage of homozygous mice with that of wild-type mice (Fig. 4). In epiphysial growth plates, the chondrocytes of the distinct differenti-

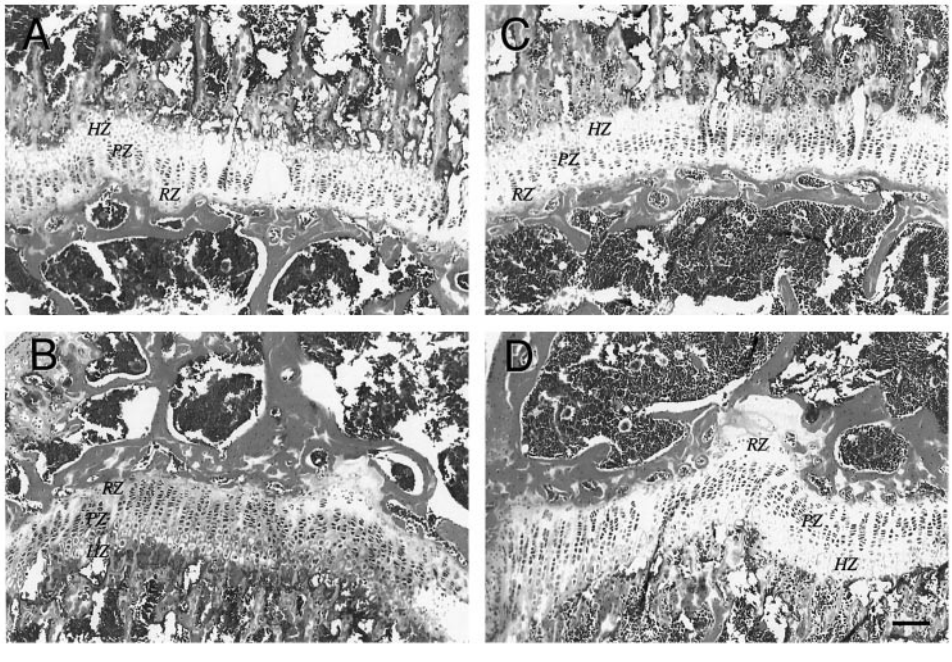

Fig. 4. Histology of epiphysial growth plates of $EDB^{-/-}$ mice. Sections of growth plates from femur (*A* and *C*) and tibia (*B* and *D*) of 5-week-old wild-type (*A* and *B*) and $EDB^{-/-}$ (*C* and *D*) mice were stained with H&E. Zones of resting (*RZ*), proliferating (*PZ*), and hypertrophic (*HZ*) chondrocytes were recognized in sections from both wild-type and mutant mice; bar, 100 μm.

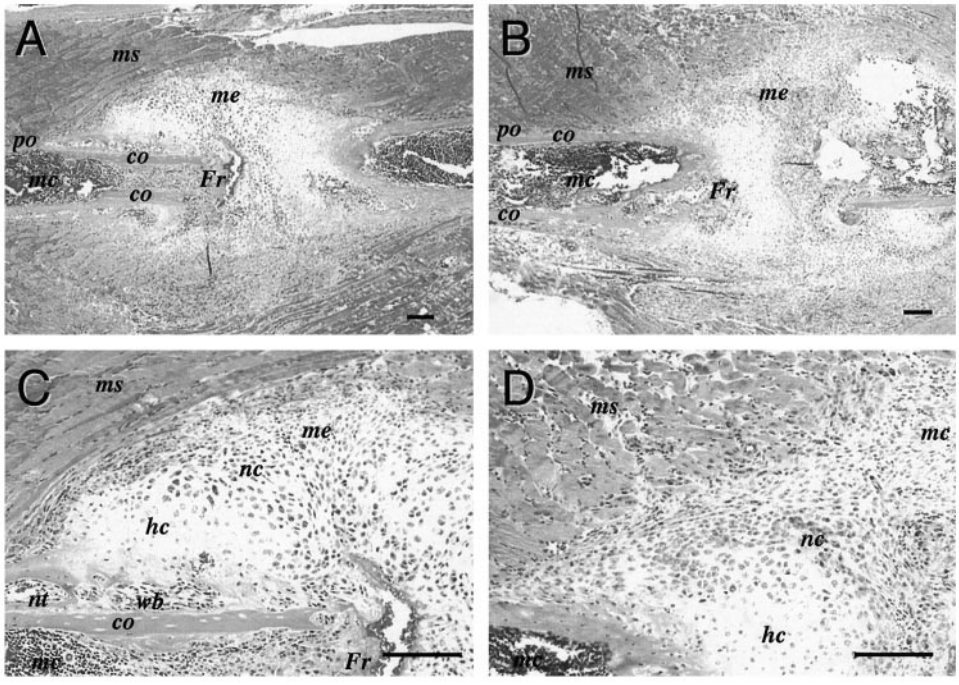

Fig. 5. Histology of rib fracture healing in EDB-deficient mice. Histological appearance of the fracture healing was compared between wild-type (*A* and *C*) and EDB-deficient (*B* and *D*) mice. The right eighth rib was surgically fractured, and the histology of the healing rib and surrounding tissues were examined 7 days after surgery as described in "Materials and Methods." Photomicrographs show the gross histology of the fracture callus at low magnification (*A* and *B*) and the magnified view focusing on the morphology of the proliferating and hypertrophic chondrocytes (*C* and *D*). *Fr*, fracture sites. Specific regions were labeled as follows: periosteum (*po*); muscle (*ms*); cortical bone (*co*); medullary cavity (*mc*); condensation of mesenchyme (*me*); primitive woven bone without trabeculae (*wb*); newly formed cartilage (*nc*); zone of hypertrophic chondrocytes (*hc*); and newly formed trabecular bone (*nt*). Bar, 200 μm.

ation stages, *i.e.*, resting, proliferating, and hypertrophic chondrocytes, are arranged in long parallel columns. Examination of the growth plates of the tibia and femur of 5-week-old homozygous mice did not show any anatomical aberration in the organization of the chondrocytes of the different differentiation stages. No clear differences were observed between wild-type and homozygous mice of different ages (*e.g.*, neonates and 6-month-old mice; data not shown). Histological aberration was also not observed in the Descemet's membrane of $EDB^{-/-}$ mice (data not shown). These data suggested that either EDB-containing FNs are not essential for the development of these tissues or that other protein(s) may compensate for the role of the EDB-containing FNs in the developmental processes.

Possible involvement of EDB-containing FNs in chondrogenic differentiation was also studied using an *in vivo* model of rib fracture healing (26). The right eighth rib of 5-week-old mice was fractured by surgery, and the process of fracture healing was examined histologically 7 days after surgery (Fig. 5). In both EDB-deficient and wild-type mice, the fracture site was bridged by a typical cartilaginous external callus containing various stages of proliferating and hypertrophic chondrocytes. The bone cortex near the fracture end was surrounded by a periosteal bony callus with trabeculae. There were no significant differences in the histology of the fracture healing process between the two genetically different groups of mice. Normal condensation of prechondrogenic mesenchymal cells was observed in the EDB-deficient mice as well as in the wild-type mice at the periphery of the external callus. These results, taken together with the normal histology of the hyaline cartilage of wild-type and homozygous mice, indicate that EDB-containing FNs, although specifically expressed in chondrogenic tissues in adult mice, are dispensable for chondrogenic differentiation in both normal development and during the bone repair process.

Reduced Growth Potential of Cultured Fibroblasts Derived from $EDB^{-/-}$ Mice. Although $EDB^{-/-}$ mice developed normally, we could not exclude the possibility that the EDB segment might be involved in the regulation of FN-dependent cellular processes by modifying FN functions. To explore this possibility, we compared the *in vitro* growth potential of fibroblasts isolated from embryos of wild-type and $EDB^{-/-}$ mice. A small but significant difference in growth rate was reproducibly observed between $EDB^{-/-}$ and $EDB^{+/+}$ fibroblasts (Fig. 6). The growth of $EDB^{-/-}$ fibroblasts was significantly slower than $EDB^{+/+}$ fibroblasts, whereas $EDB^{+/-}$ fibroblasts exhibited an intermediate growth rate between $EDB^{-/-}$ and $EDB^{+/+}$ cells, suggesting that the *in vitro* growth potential of embryonic fibroblasts might be modulated by the EDB segment of FNs.

The difference in cell growth potential between $EDB^{+/+}$ and $EDB^{-/-}$ fibroblasts could be because of a difference either in their ability to deposit FNs in the extracellular matrix or in their levels of FN expression. Indirect immunofluorescence staining of $EDB^{+/+}$ and $EDB^{-/-}$ fibroblasts with a polyclonal anti-mouse FN antibody showed that $EDB^{-/-}$ cells assembled significantly less FN matrix than $EDB^{+/+}$ cells (Fig. 7*A*). Densitometric quantitation of the immunofluorescence intensities showed that $EDB^{-/-}$ cells deposited

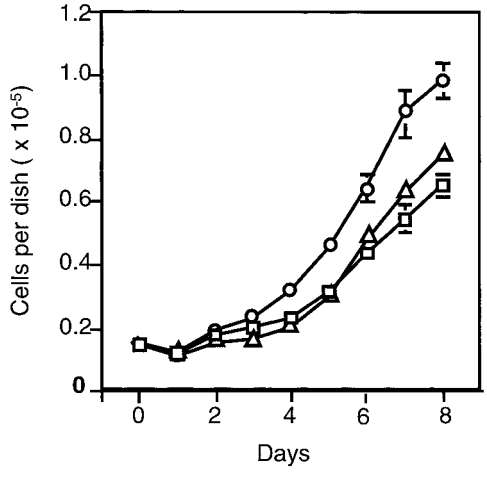

Fig. 6. Growth curve of embryonic fibroblasts. Mouse embryonic fibroblasts prepared from EDB+/+ (○), $EDB^{+/-}$ (△), and $EDB^{-/-}$ (□) mice were plated at a density of 1.5×10^4 cells/35-mm dish in DMEM supplemented with 5% FN-depleted FBS and cultured for the indicated periods. Cell numbers were determined using a Coulter counter. Each bar represents the mean SD ($n = 6$).

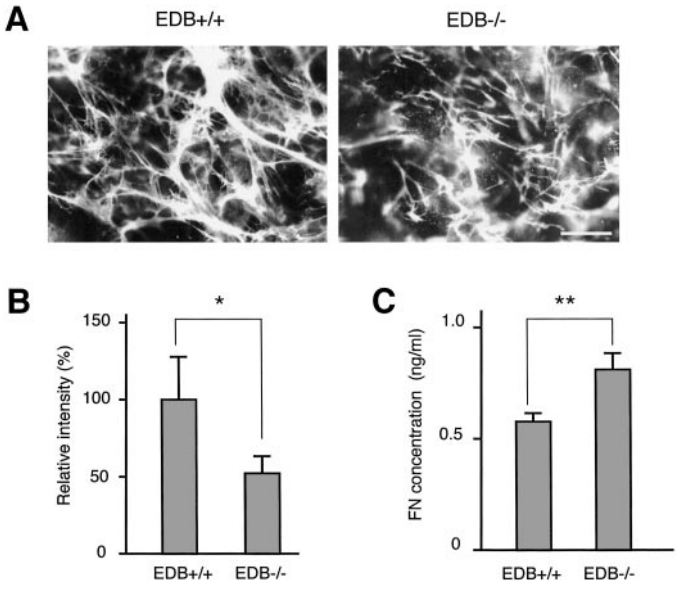

Fig. 7. Reduced FN matrix assembly in $EDB^{-/-}$ embryonic fibroblasts. *A*, fibroblasts derived from $EDB^{+/+}$ (*left*) and $EDB^{-/-}$ (*right*) mice were plated at the same density (2×10^5 cells/well) on glass coverslips and cultured for 24 h in DMEM containing 5% FN-depleted FBS. Cells were subjected to indirect immunofluorescence staining with an antimouse FN antibody as described in "Materials and Methods"; bar, 50 μm. *B*, the immunofluorescence intensities of the FN matrix were quantified using the NIH Image program. Ten separate immunofluorescence images were scanned and averaged; *, $P < 0.0001$. *C*, in parallel with the immunofluorescence staining of the FN matrix, the concentration of FN in the conditioned medium was determined by ELISA; **, $P < 0.001$.

~45% less FN matrix than $EDB^{+/+}$ cells (Fig. 7*B*). FN fibrils assembled by $EDB^{-/-}$ fibroblasts were slightly thinner and shorter than those assembled by $EDB^{+/+}$ fibroblasts. The decreased deposition of FN matrix in $EDB^{-/-}$ fibroblasts was not because of a reduction in the level of FN expression because the concentration of FNs in the conditioned medium of $EDB^{-/-}$ cells was higher than that of $EDB^{+/+}$ cells (Fig. 7*C*). Furthermore, quantitation of the levels of FN mRNA by real-time PCR did not show any significant difference between $EDB^{+/+}$ and $EDB^{-/-}$ cells (data not shown). These results, together with the normal level of plasma FN concentration in $EDB^{-/-}$ mice, indicate that the reduced FN matrix assembly of $EDB^{-/-}$ fibroblasts is because of the reduced potency of EDB-deficient FNs to assemble into the extracellular matrix.

DISCUSSION

Despite the highly regulated expression of EDB-containing FNs during embryonic development and in pathological processes, including wound healing and tumorigenesis, specific functions of the EDB segment have only been poorly defined. One approach to elucidate the function of the EDB segment is to purify homogeneous FN isoforms containing or lacking EDB and to compare their biological activities. Previously, Guan *et al.* (19) produced various alternatively spliced FNs using retroviral expression vectors and showed that there were no marked differences in their abilities to mediate cell adhesion, migration, and cytoskeletal reorganization. They also showed that EDB^+ isoforms were slightly more efficient than EDB^- isoforms at assembling into the extracellular matrix, although the EDB^+ and EDB^- isoforms used were not equivalent with respect to the other alternatively spliced regions (*i.e.*, EDA and IIICS). Recently, we produced a panel of recombinant FN isoforms covering all combinations of EDA and EDB segments and found that the cell-adhesive and integrin-binding activities of FN were significantly higher with EDA^+ isoforms than EDA^- isoforms (15, 16). No clear differences in these activities were, however, found between EDB^+ and EDB^- isoforms. No distinctive functions of EDB segment have thus far emerged from *in vitro* functional assays (15, 16, 19).

Another approach to elucidate the functions of the EDB segment is to produce animal models that cannot produce EDB^+ FN isoforms via gene knockout technology. Because conventional knockout of the FN gene in mice results in embryonic lethality (2), it is necessary to specifically eliminate the EDB exon without perturbing the level of expression of the FN gene. Georges-Labouesse *et al.* (3) constructed two targeting vectors focusing on the EDB exon, one for deletion of the EDB exon and the other for knockin of EDB. Unfortunately, both targeting constructs resulted in null mutation upon homologous recombination, failing to produce EDB exon-specific knockout or knockin mice. Abrogation of the FN expression in these mice could be because of the *neo* cassette introduced into the FN gene for selection of the homologously recombined ES cells or to partial deletion of intronic sequences downstream of the EDB exon that have been shown to be crucial for the recognition of EDB as an exon (29). To overcome these potential problems, we used a gene targeting strategy using the Cre-loxP system of bacteriophage P1. We deleted the EDB exon by two-step recombination events, *i.e.*, homologous recombination of the FN gene with the targeting vector, followed by Cre-mediated removal of the floxed EDB exon together with the *neo* cassette. One of the eight (T)GCATG repeats in the intron downstream of the EDB exon, the repeats proposed as the candidate motifs for correct splicing of EDB, was eliminated after Cre-mediated removal of the floxed EDB exon, but this did not cause any deleterious effects on the expression and/or splicing of the targeted allele, as evidenced by the normal levels of plasma FN in $EDB^{-/-}$ mice and by the comparable levels of FN expression by $EDB^{+/+}$ and $EDB^{-/-}$ embryonic fibroblasts. It should also be noted that the single loxP site left behind between exons III7b and III8a after Cre-mediated recombination did not interfere with the transcription and/or splicing of the targeted FN gene either.

Mutant mice homozygous for the EDB-deficient allele were obtained at the predicted Mendelian frequencies with two independent targeted ES clones. Furthermore, the $EDB^{-/-}$ mice developed normally and were fertile. In normal adult mice, EDB^+ FNs have been shown to be expressed only in restricted tissues such as hyaline cartilage and Descemet's membrane of cornea (14), but no histological abnormalities were detected in the articular cartilage of the femur and tibia or in cornea. No abnormalities were observed in the healing of bone fractures in $EDB^{-/-}$ mice either, supporting the conclusion that chondrocyte function during endochondral ossification was not impaired in $EDB^{-/-}$ mice. The failure to detect any developmental defects in $EDB^{-/-}$ mice, particularly in the process of ossification, does not seem to be because of variation in the genetic background because no abnormalities were detectable in homozygous mice either with the chimeric background of 129 and C57 strains or after repeated backcrossing with 129 strain. No apparent behavioral abnormalities were observed with $EDB^{-/-}$ mice either, although we cannot exclude the possibility that $EDB^{-/-}$ mice manifest aberrant behavior upon pathological intervention, as has been shown for the tenascin knockout mice (30).

EDB^+ FNs have been shown to be expressed under pathological conditions such as tissue repair and tumorigenesis (31). In malignant tumors as well as tumor xenografts in nude mice, EDB^+ FNs are deposited in the tumor stroma and more prominently in neovasculature within the tumor (11, 28, 32). EDB^+ FNs have therefore been proposed as a marker of angiogenesis because EDB^+ FN is expressed not only in tumor neovasculature but also in the superficial layer of the endometrium where angiogenesis occurs physiologically (27, 28). Furthermore, injection of anti-EDB antibodies labeled with ^{125}I or an

infrared fluorophore into tumor-bearing mice resulted in selective accumulation at the tumor foci (33, 34), raising the possibility that EDB^+ FNs could be used as a marker for tumor targeting. In support of this possibility, an anti-EDB antibody fused with a tissue factor, a coagulation-inducing protein, was successfully used to target the tissue factor to tumor xenografts in mice, thereby inducing selective infarction of different types of solid tumors followed by complete eradication of tumors in 30% of the mice treated (35). Despite these observations, we could not find any defects in organogenesis in which extensive angiogenesis/vasculogenesis are closely associated. No anatomical abnormalities were observed in the lung and kidney, the organs with extensive microvasculature. Close association of EDB^+ FN expression with various types of tumors (11, 32, 36) may imply a role of EDB^+ FN in tumorigenesis, but no clear evidence supporting this possibility has ever been obtained. We have crossed $EDB^{-/-}$ mice with p53-null mice to generate double knockout mice lacking the EDB exon and a functional *p53* gene. However, no clear difference in the length of survival periods was observed between $EDB^{-/-}p53^{-/-}$ and $EDB^{+/+}p53^{-/-}$ mice,[8] arguing against the possibility that expression of EDB^+ FNs potentiates tumor growth and/or tumor angiogenesis.

Although no clear function of EDB^+ FNs emerged from the *in vivo* studies of EDB-null mice, embryonic fibroblasts prepared from $EDB^{-/-}$ mice proliferated more slowly than those from $EDB^{+/+}$ mice *in vitro*. Furthermore, fibroblasts from $EDB^{-/-}$ mice produced FN fibrils that were shorter and thinner than those deposited by $EDB^{+/+}$ fibroblasts. These differences were not dramatic but were reproducible in separate experiments. In support of these observations, recombinant rat FN containing either the EDA or EDB segment was more readily incorporated into existing FN matrices than those lacking these extra domains (19). In explant culture of articular cartilage, EDB^+ FNs produced by cultured chondrocytes were preferentially retained in the cartilage matrix rather than exported to the culture medium (37), suggesting a role of the EDB segment in FN matrix assembly in cartilage. Consistent with this observation, immunohistochemical analysis of the articular cartilage showed that $EDB^{-/-}$ mice deposited significantly less FN in the cartilage matrix than $EDB^{+/+}$ mice.[9] These results, taken together, indicate that expression of EDB^+ FNs may play a regulatory role in FN matrix assembly and proliferation of connective tissue cells. Given that matrix-assembled FNs transduce signals that stimulate cell cycle progression via integrin $\alpha5\beta1$ and some other Arg-Gly-Asp (RGD)-recognizing integrin(s) (38), decreased FN matrix assembly may well explain the reduced proliferative potential of $EDB^{-/-}$ fibroblasts *in vitro*. Nevertheless, neither growth retardation nor malformation of specific organs was detectable with $EDB^{-/-}$ mice, arguing against a regulatory role for EDB^+ FNs in cell proliferation *in vivo*. Apparent normalcy of $EDB^{-/-}$ mice, however, does not exclude the possibility that EDB^+ FNs may play a role in cell proliferation in some pathological processes. Although EDB^+ FN deficiency does not have any discernible effects on bone fracture healing or in tumorigenesis associated with ablation of the p53 tumor suppressor gene, the search for distinctive phenotypes of $EDB^{-/-}$ mice needs to be continued to uncover the *in vivo* function of EDB^+ FNs in normal and pathological processes.

In summary, we generated mice deficient in the EDB exon using the Cre-loxP recombination system. Unexpectedly, the homozygous $EDB^{-/-}$ mice grew normally and were fertile without showing any distinctive phenotypes, despite the restricted expression pattern of EDB^+ FNs during embryogenesis and in normal adult tissues. Although *in vivo* function(s) of EDB^+ FNs therefore remains to be elucidated, embryonic fibroblasts prepared from $EDB^{-/-}$ mice exhibited discernible differences from $EDB^{+/+}$ fibroblasts in their ability to proliferate *in vitro* and to assemble FN matrices, indicating the possibility that the EDB segment may play a role in the regulation of FN matrix assembly and FN matrix-dependent cell growth. Given the exceptionally conserved amino acid sequence of the EDB segment between different species, *i.e.*, 100% homology between human, rat, and mouse and 97% homology between human and chicken, it is important to continue the pursuit of the function(s) of EDB^+ FNs by pathological intervention, as was successfully demonstrated with tenascin-C knockout mice. The $EDB^{-/-}$ mice developed should provide a valuable model to uncover hitherto unknown function(s) of the highly conserved EDB segment.

[8] T. Fukuda and K. Sekiguchi, unpublished observation.

[9] Y. Mizuno-Horikawa and K. Sekiguchi, unpublished observation.

ACKNOWLEDGMENTS

We thank Dr. Klaus Rajewsky for the generous gifts of the floxed *neo* gene and pCI-Cre, Dr. Takashi Tanaka for comments on the targeting vector construction, and Noriko Sanzen, Miho Ujikawa, and Teruko Iwaki for their expert technical assistance.

REFERENCES

1. Hynes, R. O. Fibronectin. New York: Springer-Verlag, 1990.
2. George, E. L., Georges-Labouesse, E. N., Patel-King, R. S., Rayburn, H., and Hynes, R. O. Defects in mesoderm, neural tube and vascular development in mouse embryos lacking fibronectin. Development (Camb.), *119:* 1079–1091, 1993.
3. Georges-Labouesse, E. N., George, E. L., Rayburn, H., and Hynes, R O. Mesodermal development in mouse embryos mutant for fibronectin. Dev. Dyn., *207:* 145–156, 1996.
4. Petersen, T. E., Thogersen, H. C., Skorstengaard, K., Vibe-Pedersen, K., Sahl, P., Sottrup-Jensen, L., and Magnusson, S. Partial primary structure of bovine plasma fibronectin: three types of internal homology. Proc. Natl. Acad. Sci. USA, *80:* 137–141, 1983.
5. Schwarzbauer, J. E., Tamkun, J. W., Lemischka, I. R., and Hynes, R. O. Three different fibronectin mRNA arise by alternative splicing within the coding region. Cell, *35:* 421–431, 1983.
6. Kornblihtt, A. R., Vibe-Pedersen, K., and Baralle, F. E. Human fibronectin: cell specific alternative mRNA splicing generates polypeptide chains differing in the number of internal repeats. Nucleic Acids Res., *12:* 5853–5868, 1984.
7. Zardi, L., Carnemolla, B., Siri, A., Petersen, T. E., Paolella, G., Sebastio, G., and Baralle, F. E. Transformed human cells produce a new fibronectin isoform by preferential alternative splicing of a previously unobserved exon. EMBO J., *6:* 2337–2342, 1987.
8. Schwarzbauer, J. E., Patel, R. S., Fonda, D., and Hynes, R. O. Multiple sites of alternative splicing of the rat fibronectin gene transcript. EMBO J., *6:* 2573–2580, 1987.
9. Oyama, F., Hirohashi, S., Shimosato, Y., Titani, K., and Sekiguchi, K. Deregulation of alternative splicing of fibronectin pre-mRNA in malignant human liver tumors. J. Biol. Chem., *264:* 10331–10334, 1989.
10. Oyama, F., Murata, Y., Suganuma, N., Kimura, T., Titani, K., and Sekiguchi, K. Patterns of alternative splicing of fibronectin pre-mRNA in human adult and fetal tissues. Biochemistry, *28:* 1428–1434, 1989.
11. Carnemolla, B., Balza, E., Siri, A., Zardi, L., Nicotra, M. R., Bigotti, A., and Natali, P. G. A tumor-associated fibronectin isoform generated by alternative splicing of messenger RNA precursors. J. Cell Biol., *108:* 1139–1148, 1989.
12. Ffrench-Constant, C., and Hynes, R. O. Alternative splicing of fibronectin is temporally and spatially regulated in the chicken embryo. Development (Camb.), *106:* 375–388, 1989.
13. Oyama, F., Hirohashi, S., Sakamoto, M., Titani, K., and Sekiguchi, K. Coordinate oncodevelopmental modulation of alternative splicing of fibronectin pre-messenger RNA at ED-A, ED-B, and CS1 regions in human liver tumors. Cancer Res., *53:* 2005–2011, 1993.
14. Peters, J. H., Chen, G. E., and Hynes, R. O. Fibronectin isoform distribution in the mouse. II. Differential distribution of the alternatively spliced EIIIB, EIIIA, and V segments in the adult mouse. Cell Adhes. Commun., *4:* 127–148, 1996.
15. Manabe, R., Oh-e, N., Maeda, T., Fukuda, T., and Sekiguchi, K. Modulation of cell-adhesive activity of fibronectin by the alternatively spliced EDA segment. J. Cell Biol., *139:* 295–307, 1997.
16. Manabe, R., Oh-e, N., and Sekiguchi, K. Alternatively spliced EDA segment regulates fibronectin-dependent cell cycle progression and mitogenic signal transduction. J. Biol. Chem., *274:* 5919–5924, 1999.
17. Jarnagin, W. R., Rockey, D. C., Koteliansky, V. E., Wang, S. S., and Bissell, D. M. Expression of variant fibronectins in wound healing: cellular source and biological activity of the EIIIA segment in rat hepatic fibrogenesis. J. Cell Biol., *127:* 2037–2048, 1994.

18. Saito, S., Yamaji, N., Yasunaga, K., Saito, T., Matsumoto, S., Katoh, M., Kobayashi, S., and Masuho, Y. The fibronectin extra domain A activates matrix metalloproteinase gene expression by an interleukin-1-dependent mechanism. J. Biol. Chem., *274:* 30756–30763, 1999.
19. Guan, J. L., Trevithick, J. E., and Hynes, R. O. Retroviral expression of alternatively spliced forms of rat fibronectin. J. Cell Biol., *110:* 833–847, 1990.
20. Sauer, B., and Henderson, N. Site-specific DNA recombination in mammalian cells by the Cre recombinase of bacteriophage P1. Proc. Natl. Acad. Sci. USA, *85:* 5166–5170, 1988.
21. Gu, H., Marth, J. D., Orban, P. C., Mossmann, H., and Rajewsky, K. Deletion of a DNA polymerase β gene segment in T cells using cell type specific gene targeting. Science (Wash. DC), *265:* 103–106, 1994.
22. Hedman, K., Kurkinen, M., Alitalo, K., Vaheri, A., Johansson, S., and Hook, M. Isolation of the pericellular matrix of human fibroblast cultures. J. Cell Biol., *81:* 83–91, 1979.
23. Laemmli, U. K. Cleavage of structural proteins during the assembly of the head of the bacteriophage T4. Nature (Lond.), *227:* 680–685, 1970.
24. Sekiguchi, K., and Titani, K. Probing molecular polymorphism of fibronectin with antibodies directed to the alternatively spliced peptide segment. Biochemistry, *28:* 3293–3298, 1989.
25. Kagan, A., and Glick, M. Oxytocin. *In:* B. M. Jaffe and H. R. Behrman (eds.), Methods of Hormone Radioimmunoassay, pp. 327–339. New York: Academic Press, 1979.
26. Nakase, T., Nomura, S., Yoshikawa, H., Hashimoto, J., Hirota, S., Kitamura, Y., Oikawa, S., Ono, K., and Takaoka, K. Transient and localized expression of bone morphogenetic protein 4 messenger RNA during fracture healing. J. Bone Miner. Res., *9:* 651–659, 1994.
27. Castellani, P., Viale, G., Dorcaratto, A., Nicolo, G., Kaczmarek, J., Querze, G., and Zardi, L. The fibronectin isoform containing the ED-B oncofetal domain: a marker of angiogenesis. Int. J. Cancer, *59:* 612–618, 1994.
28. Carnemolla, B., Neri, D., Castellani, P., Leprini, A., Neri, G., Pini, A., Winter, G., and Zardi, L. Phage antibodies with pan-species recognition of the oncofetal angiogenesis marker fibronectin ED-B domain. Int. J. Cancer, *68:* 397–405, 1996.
29. Huh, G. S., and Hynes, R. O. Regulation of alternative pre-mRNA splicing by a novel repeated hexanucleotide element. Genes Dev., *8:* 1561–1574, 1994.
30. Mackie, E. J., and Tucker, R. P. The tenascin-C knockout revisited. J. Cell Biol., *112:* 3847–3853, 1999.
31. Ffrench-Constant, C. Alternative splicing of fibronectin: many different proteins but few different functions. Exp. Cell Res., *221:* 261–271, 1995.
32. Kaczmarek, J., Castellani, P., Nicolo, G., Spina, B., Allemanni, G., and Zardi, L. Distribution of oncofetal fibronectin isoforms in normal hyperplastic and neoplastic human breast tissues. Int. J. Cancer, *58:* 11–16, 1994.
33. Fattorusso, R., Pellecchia, M., Viti, F., Neri, P., Neri, D., and Wuthrich, K. NMR structure of the human oncofetal fibronectin ED-B domain, a specific marker for angiogenesis. Structure (London), *7:* 381–390, 1999.
34. Mariani, G., Lasku, A., Balza, E., Gaggero, B., Motta, C., Di Luca, L., Dorcaratto, A., Viale, G. A., Neri, D., and Zardi, L. Tumor targeting potential of the monoclonal antibody BC-1 against oncofetal fibronectin in nude mice bearing human tumor implants. Cancer (Phila.), *80:* 2378–2384, 1997.
35. Nilsson, F., Losmehl, H., Zardi, L., and Neri, D. Targeted delivery of tissue factor to the ED-B domain of fibronectin, a marker of angiogenesis, mediates the infarction of solid tumors in mice. Cancer Res., *61:* 711–716, 2001.
36. Midulla, M., Verma, R., Pignatelli, M., Ritter, M. A., Courtenay-Luck, N. S., and George, A. J. T. Source of oncofetal ED-B-containing fibronectin: implications of production by both tumor and endothelial cells. Cancer Res., *60:* 164–169, 2000.
37. Zang, D. W., Burton-Wurster, N., and Lust, G. Antibody specific for extra domain B of fibronectin demonstrates elevated levels of both extra domain B(+) and B(-) fibronectin in osteoarthritic canine cartilage. Matrix Biol., *14:* 623–633, 1995.
38. Assoian, R. K., and Schwartz, M. A. Coordinate signaling by integrins and receptor tyrosine kinases in the regulation of G_1 phase cell-cycle progression. Curr. Opin. Genet. Dev., *11:* 48–53, 2001.